2021 IEEE Intl Conf on Parallel & Distributed Processing with Applications, Big Data & Cloud Computing, Sustainable Computing & Communications, Social Computing & Networking (ISPA/BDCloud/SocialCom/SustainCom)

Efficient Wireless Static Chargers Deployment for UAV Networks

Mengqi Li, Liang Liu, Yanlin Wang, Jianfei Peng, Jie Xi, Lisong Wang
College of Computer Science and Technology
Nanjing University of Aeronautics and Astronautics
Nanjing, China
{mengqili, liangliu, wangyanlin1997, pengjf, miracle, wangls}@nuaa.edu.cn

***Abstract*—To prolong the lifetime of unmanned aerial vehicle (UAV) networks, this paper studies how to efficiently deploy wireless static chargers (WSCs) in UAV networks (WDU). That is, given a set of UAVs, determining the minimum number of WSCs as well as the location of each WSC, so that UAVs do not run out of energy during flight. We first formulate WDU as an optimization problem, which is proved to be NP-hard. Then to solve WDU, we propose the scheme of selecting WSCs' locations by transforming WDU into a binary integer programming (BIP) problem (SLTB). In SLTB, we first propose a novel area discretization method to reduce the solution space of WDU, and then WDU is reformulated as a BIP problem that can be easily solved by existing methods. Finally, experiments are conducted to evaluate the performance of SLTB in terms of reducing the number of WSCs.**

***Index Terms*—UAV network, UAV charging, wireless charging, charger deployment**

I. Introduction

Due to the portability and flexibility of UAVs, multiple UAVs are coordinated as a UAV network to execute tasks in many fields [15], such as agriculture, military, transportation, and so on. In UAV networks, the ground base station (GS) plans the flight path of each UAV according to path planning algorithms [27]–[29], and each UAV flies along its pre-planned flight path to execute the pre-assigned task. The energy capacity of UAVs is limited [16], and once a UAV runs out of energy, the task of the entire UAV network may fail.

To solve this problem, there are some works dedicated to studying how to replenish energy for UAVs during the flight [17], [18]. For example, some works attempt to replenish energy for UAVs with natural energy [7], such as wind energy, solar energy, and so on. To provide a stable energy supplement, the contact-based ground charging platform is proposed [17], in which UAVs need to suspend the task first, then land on the ground charging platform to replenish energy, and finally take off again to continue the task.

Motivations: The method of charging UAVs on the ground charging platform has many drawbacks. Firstly, the deployment cost of the charging platform is very expensive [9]. Secondly, charging on the platform is inefficient. This is because UAVs that need to replenish energy have to land first and wait until the charging is completed. Therefore, when there are many low-energy UAVs, the queue of requesting charging may become longer and the time for UAVs to wait for charging becomes longer.

In recent years, wireless power transmission technology (WPT) is proposed and has been widely studied to charge UAVs wirelessly [30]–[32]. For example, the Air TurnKey wireless charging system [30] proposed by GET can charge multiple UAVs in flight within a range of 10m with an average charging efficiency of 80%. A big commercial UAV can be fully charged in 6 minutes efficiently, then it can continue to fly for 20-40 minutes. GET claims that the wireless charging range can reach more than 20 meters by 2021.

Based on this, we attempt to deploy the least wireless static chargers (WSCs) in UAV networks to realize charging UAVs while flying, so that the taking-off and landing time can be saved and the deployment cost can be minimized.

Challenges: Under the premise that UAVs can replenish energy they need, to determine the minimum number of WSCs as well as the location of each WSC, we propose the problem of WSC deployment in UAV networks (WDU). Solving WDU is not trivial, and there are three challenges. Firstly, the number of locations where we can place WSCs is infinite. Secondly, unlike other static networks in which the rechargeable devices are static, the flight paths of UAVs are continuous and the positions of UAVs change continuously. It's hard to guarantee UAVs do not run out of energy in each position.

Contributions: The contributions of this paper are summarized as follows:

1) In order to ensure that UAVs can replenish the energy they need so that UAV networks can complete the long-time tasks, we propose the WDU problem and formalize it as an optimization problem.

2) To solve WDU, we propose the scheme of selecting WSCs' locations by transforming WDU into a binary integer programming (BIP) problem (SLTB). In SLTB, we present a novel area discretization method to reformulate WDU as a BIP problem that can be solved by existing methods.

3) Finally, experiments are conducted to evaluate the performance of SLTB in saving the number of deployed WSCs.

Our scheme SLTB solves the challenges by area discretization. The area discretization we proposed in this paper not only makes the locations where WSCs can be placed finite but also makes the locations where UAVs can be charged finite. In addition, SLTB determines the minimal number of WSCs and

978-0-7381-2646-3/21/$31.00 ©2021 IEEE

DOI 10.1109/ISPA-BDCloud-SocialCom-SustainCom52081.2021.00200

the location of each WSC by reformulating WDU as a BIP problem.

Compared with the charger deployment in static networks [1]–[6], this paper solves the problem of charger deployment in dynamic UAV networks in which the rechargeable devices are mobile. In addition, compared with [12], [13], the WSCs in our scheme can be placed at any location in the UAV network by adjusting the discretization granularity. Finally, the charging power in our scheme is inversely proportional to the square of the distance, which is more realistic than the charging model in [13].

Organization: The rest of this paper is organized as follows: we investigate related work in Section II. Section III introduces the network model, charging model, and problem statement. We introduce our scheme SLTB in section IV. Experimental results and conclusions are provided in Section V and Section VI.

II. Related work

According to whether the rechargeable devices can move, existing researches on static charger deployment can be divided into two types.

A. Charger Deployment in Static Network

In static networks, the location of each rechargeable device is fixed. [1] introduces the traditional Greedy Cone Covering (GCC) algorithm, which greedily deploys chargers to charge the static sensor nodes in the network. To gain positions of chargers over the local optimal result, the globally optimal result and make WRSNs sustainable by adjusting the locations of chargers, [2] proposes the PSCD (Particle Swarm Charger Deployment) algorithm to optimize WRSN charger deployment. To guarantee the EMR Safety for every location on the plane, [3] discretizes the placement area into many grids and proposes an approximate algorithm to deploy chargers.

Unlike these studies, the deployment of directional chargers is considered in [4]. [4] studies the problem of placing directional wireless chargers to determine deployment locations, orientations, and portions of time for all chargers such that the overall charging utility of all devices can be maximized. Considering the limited communication range of multiple directional chargers, [5] proposes an algorithm with a constant approximation ratio to determine the placement locations and directions of wireless chargers under connection constraints. Unlike previous studies, the deployment of a mixture of directional and omnidirectional chargers is considered in [6], which proposes a method to find the minimal number of chargers to cover all sensor nodes in the WRSNs.

In the above studies, the rechargeable devices are static. When the locations of the WSCs are determined, the energy that the static devices can receive is determined. However, in UAV networks, the location of each UAV is continuously changing, and the energy that each UAV can receive is different at different moments. Therefore, the charger deployment methods in the static network do not apply to the WSCs deployment in UAV networks.

B. Charger Deployment in Dynamic Network

In dynamic networks, the rechargeable devices are mobile, so when the locations of WSCs are determined, the power received by the rechargeable devices is changeable. Both [8] and [9] consider the charger deployment problem with mobile rechargeable devices. Full coverage charger deployment is discussed in [8] and it is assumed that terminal devices are evenly distributed in the covered area. Instead, [9] aims to achieve high network survival through a more realistic partial coverage approach, taking into account the human mobility of carrying terminal devices in extremely large sensor networks. Based on the more complicated mobility pattern of people who wear wearable devices, [10] formulates the problem which investigates a specific stay-move behavior pattern to deploy a charger to minimize the charging service budget. Compared with [10], the deployment of one charger is further extended to multiple chargers in [11] to monitor the energy consumption of wearable devices in real-time.

Although the above researches take into account the mobility of rechargeable devices and the deployment of WSCs can cover all areas where devices may appear, it ignores the energy that the rechargeable devices required actually and fails to charge on demand. Based on the actual energy required by UAVs, this paper proposes a scheme to deploy WSCs. On the premise of UAVs can be replenished with required energy, WSCs are deployed as little as possible to save energy consumption of the UAV network.

III. Preliminaries

In this section, we introduce the network model, the charging model, and the problem statement. The related symbols and definitions are shown in Table I.

TABLE I: Symbols and Definitions

Symbols	Definitions
N	The number of UAVs
u_i	The i-th UAV
$d(a,b)$	The distance between locations a and b
α, β	The charging parameters
T_i	The flight time of u_i
re_i^t	The remaining energy of u_i at time t
E_d	The dropping energy threshold of UAVs
E_c	The energy capacity of UAVs
E_0	The initial energy of UAVs
μ	The energy consumption rate of UAVs
v	The flight speed of UAVs
Ω	The WSCs placement area
$\|G\|$	The number of all discrete grids in Ω
g_j	The j-th grid in Ω
o_j	The center of g_i
g_i^k	The k-th path grid of u_i
T_i^k	The flight time period of u_i in g_j^k
$g_{i,j}^m$	The m-th rechargeable path grid of u_i about g_j
$inT_{i,j}^m$	The rechargeable flight time period in $g_{i,j}^m$

A. Network Model

As shown in the Fig. 1, after GS plans the flight paths of UAVs according to the path planning algorithms [27]–[29],

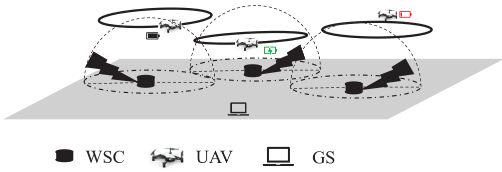

Fig. 1: The UAV network

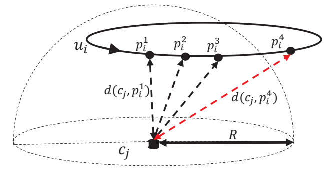

Fig. 2: Charging model

N UAVs $\{u_1, u_2, \cdots, u_N\}$ fly along the pre-planned flight paths. In this paper, WSCs adopt omnidirectional charging [1], namely, the charging range of each WSC is a circle and all UAVs within the charging circle can be charged. Furthermore, we consider the many-to-many charging model [23], that is, a UAV can receive energy from multiple WSCs at one location, and a WSC can charge multiple UAVs within its range simultaneously.

B. Charging Model

This paper adopts the WISP-reader charging model [25]. The charging power received by the rechargeable devices can be calculated as:

$$Pr(c,p) = \frac{G_s G_r \eta}{L_p} \left(\frac{\lambda}{4\pi \left(d(c,p) + \beta\right)} \right)^2 P_0 \tag{1}$$

where $d(c,p)$ is the Euclidean distance between the location of charger c and location p where the rechargeable device stays. P_0 is the source power of chargers, G_s is the source antenna gain, G_r is the receive antenna gain, L_p is polarization loss, λ is the wavelength, η is rectifier efficiency, and β is a parameter to adjust the Frris' free space equation for short-distance transmission.

In one-to-many charging model [23], assuming the maximum charging radius of chargers is R [26], when there are multiple UAVs close to a WSC within R, all these UAVs can be charged simultaneously. In (1), except the parameter $d(c,p)$, the rest are all constants determined by the environment or device, so we merge all these constants into α. Assuming o_c is the location of WSC c and o_i is the location of UAV u_i, (1) can be simplified as:

$$Pr\left(o_c, o_i\right) = \begin{cases} \dfrac{\alpha}{(d(o_c, o_i) + \beta)^2}, & d(o_c, o_i) \le R \\ 0 & , d(o_c, o_i) > R \end{cases} \tag{2}$$

As shown in Fig. 2, UAV u_i flies along its flight path and passes through positions $p_i^1, p_i^2, p_i^3, p_i^4$. Assuming that the charging radius of WSC c_j is R, when u_i reaches at position p_i^1, the distance between u_i and c_j is $d(c_j, p_i^1) \le R$, so u_i can receive energy from c_j and the charging power $Pr(c_j, p_i^1) > 0$. However, when u_i arrives at position p_i^4, the distance between u_i and c_j is $d(c_j, p_i^4) > R$, then u_i cannot receive energy from c_j, that is, $Pr(c_j, p_i^4) = 0$. In addition, if u_i is within the charging circles of multiple WSCs $\{c_1, c_2, \cdots, c_M\}$ at location o_i, the total charging power $Pr(o_i)$ of u_i received at location o_i is the sum of the charging power received from each WSC, that is:

$$Pr(o_i) = \sum_{m=1}^{M} Pr(c_m, o_i) \tag{3}$$

C. Problem Formulation

The goal of this paper is to determine the minimum number of WSCs as well as the location of each WSC, so that UAVs do not run out of energy during the flight. Assuming the number of WSCs that are placed in the UAV network is Ψ, the problem of WSC deployment in the UAV network (WDU) can be formalized as follows:

(P1)

$$\min \Psi \tag{4}$$

subject to:

$$\forall i \le N, t \le T_i, E_d \le re_i^t \le E_c \tag{5}$$

The condition in (5) ensures that the remaining energy re_i^t of any UAV $u_i (1 \le i \le N)$ at any time $t (t \le T_i)$ is greater than the dropping energy threshold E_d and less than the energy capacity E_c. T_i is time when u_i finishes flight.

IV. Solution

As proved in [9], the charger deployment problem with mobile devices is NP-hard. In this section, we introduce the scheme SLTB (selecting locations by transforming WDU into BIP).

A. Discretizaion

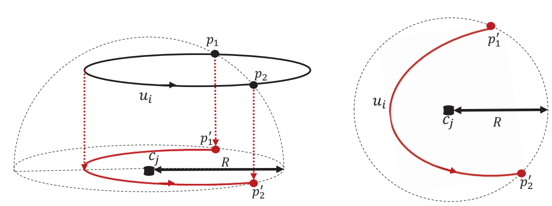

(a) The flight path in 3D (b) The flight path in 2D

Fig. 3: Mapping flight paths from 3D to 2D plane

In a UAV network, there are infinite locations where WSCs can be placed. Supposing the flight paths of UAVs are pre-planned by path planning algorithms [27]–[29], to get the

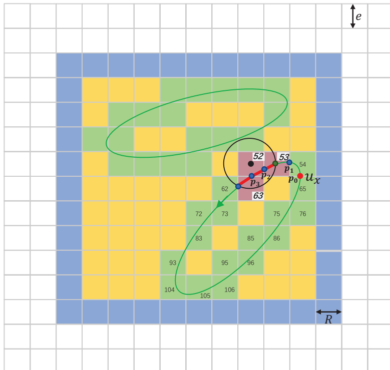

Fig. 4: Discretizaion

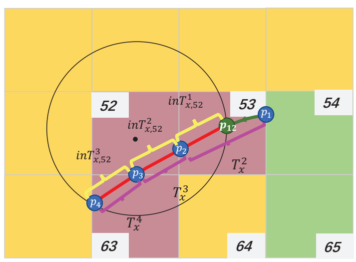

Fig. 5: Discretizaion in detail

candidate placement locations of WSCs, we discretize the placement area of WSCs and the flight paths of UAVs. Without loss of generality, we first map the flight path of u_i from 3D to 2D to determine whether the flight path of u_i is within the charging circle of WSC c_j. As shown in Fig. 3a, the positions p_1, p_2 where u_i arrives at and leaves the charging circle of c_j are mapped as $p_1^{'}$ and $p_2^{'}$. Fig. 3b shows the flight path of u_i in 2D plane.

Placement area: The area that covers all flight paths of all UAVs is defined as the flight area. Then, we uniformly expanding the flight area by the charging range of WSCs R along horizontal and vertical directions to get the **placement area** Ω of WSCs (the blue and yellow areas in Fig. 4). This is because the WSCs that are placed outside the placement area cannot replenish energy to any UAV within the flight area. Finally, to determine the candidate locations of WSCs, we discretize the placement area into many grids with the side length e. The grid set $G = \{g_1, g_2, \cdots, g_{|G|}\}$ corresponds to each discrete grid in Ω. The WSCs can be placed in the center of each grid $g_j (1 \le j \le |G|)$, and the center of each grid is denoted as o_j.

Path grids g_i^k: Supposing the number of grids that the flight path of UAV u_i passes through is K_i (as the green grids shown in Fig. 4). We call the K_i grids that UAV u_i passed as **path girds**, which are denoted as $G_i = \{g_i^1, g_i^2, \cdots, g_i^{K_i}\}$. The flight time period of u_i in each path grid $g_i^k (1 \le k \le K_i)$ is $T_i^k = [st_i^k, et_i^k]$, where st_i^k is the time when u_i enters g_i^k and et_i^k is the time when u_i leaves g_i^k.

As shown in Fig. 4, there are 121 grids in Ω. Assuming the UAV $u_x (1 \le x \le N)$ starts at position p_0. Then u_x arrives at position p_1 at time t_1, and u_x reaches at locations p_2, p_3 at time t_2 and t_3. The grid g_{54} that the flight path from p_0 to p_1 locates at is the first path grid g_x^1 of u_x. The grid g_{53} that the flight path from p_1 to p_2 locates at is the 2-nd path grid g_x^2 of u_x, that is $g_x^2 = g_{53}$. The flight time from t_1 to t_2 is denoted as the flight time period $T_x^2 = [t_1, t_2]$. Similarly, the flight path from p_2 to p_3 locates at grid g_{52}, which is the 3-rd path grid of u_x, that is $g_x^3 = g_{52}$ and $T_x^3 = [t_2, t_3]$.

Rechargeable path grids $g_{i,j}^m$: When a WSC c_j is placed in the j-th grid g_j, the sub-path of u_i that is within the charging range of c_j covers $M_{i,j}$ grids. In these $M_{i,j}$ grids, u_i can receive energy from the WSC in g_j. These path grids are called as the **rechargeable path grids** of u_i about g_j and are denoted as $G_{i,j} = \{g_{i,j}^1, \cdots, g_{i,j}^{M_{i,j}}\}$. Corresponding to each rechargeable path grid $g_{i,j}^m (1 \le m \le M_{i,j})$, the rechargeable flight time period of u_i about g_j is denoted as $reT_{i,j}^m = [sreT_{i,j}^m, ereT_{i,j}^m]$. $sreT_{i,j}^m$ and $ereT_{i,j}^m$ are the time for u_i to enter and leave the charging range of c_j when u_i flies in $g_{i,j}^m$.

It should be pointed out that, each rechargeable path grid $g_{i,j}^m (1 \le m \le M_{i,j})$ of u_i about g_j corresponds to a path grid in path grid set G_i. That is there is a grid $g_i^k \in K_i$, $g_i^k = g_{i,j}^m$. In addition, the rechargeable flight time period $reT_{i,j}^m$ corresponding to $g_{i,j}^m$, and the flight time period T_i^k corresponding g_i^k meet the following inequality: $|T_i^k| \ge |reT_{i,j}^m|$.

Taking Fig. 4 as an example, the path grid set G_x of u_x contains 19 path grids (pink and green grids). Assuming that a WSC is placed in the 52-th grid g_{52} and $R = e$. As shown in Fig. 5, there are 3 rechargeable path grids of u_x about g_{52} (pink grids in Fig. 5). The first path grid $g_x^1 = g_{54}$ is outside the charging circle of the WSC in g_{52}, and the 2-nd, 3-rd, 4-th path grids g_x^2, g_x^3, g_x^4 of u_x are within the charging circle, which correspond to the grids g_{53}, g_{52}, g_{63} in Ω.

As shown in Fig. 5, when u_x arrives at p_1 at time t_1, u_x enters the first rechargeable path grid $g_{x,52}^1$ about g_{52}. However, until at the time t_{12} when u_x arrives at p_{12}, u_x enters the charging circle and it can receive energy from the WSC in g_{52}. When u_x arrives at p_2 at time t_2, u_1 leaves $g_{x,52}^1$. Therefore, although the flight time period of u_x within the path grid g_x^2 is $T_x^2 = [t_1, t_2]$, the rechargeable time period when u_x can receive energy is $reT_{x,52}^1 = [t_{12}, t_2]$. Apparently $|reT_{x,52}^1| \le |T_x^2|$.

Similarly, we can obtain the rechargeable flight path grid set $G_{x,52}$ of UAV u_x about grid g_{52} and the corresponding rechargeable flight time period set $reT_{x,52}$ are:

$$\begin{aligned} G_{x,52} &= \{g_{x,52}^1, g_{x,52}^2, g_{x,52}^3\} \\ &= \{g_x^2, g_x^3, g_x^4\} \\ &= \{g_{53}, g_{52}, g_{63}\} \end{aligned}$$

$$\begin{aligned} reT_{x,52} &= \{reT_{x,52}^1, reT_{x,52}^2, reT_{x,52}^3\} \\ &= \{[t_{12}, t_2], [t_2, t_3], [t_3, t_4]\} \end{aligned}$$

When a WSC is placed in g_j, in order to calculate the energy that UAV $u_i (1 \le i \le N)$ received from the WSC in g_j, we approximate the charging power of u_i in each path grid $g_{i,j}^m$ as:

$$Pr\left(o_j, o_{i,j}^m\right) = \begin{cases} \dfrac{\alpha}{(d(o_j, o_{i,j}^m) + \beta)^2}, d(o_j, o_{i,j}^m) \le R \\ 0 \qquad , d(o_j, o_{i,j}^m) > R \end{cases} \tag{6}$$

where o_j is the center of grid g_j, $o_{i,j}^m$ is the center of the m-th rechargeable path grid $g_{i,j}^m$ of u_i about g_j.

Thus, the energy $\Delta E_{i,j}^m$ received by UAV u_i in $g_{i,j}^m$ from the WSC in grid g_j is equal to the charging power $Pr(o_j, o_{i,j}^m)$ times the length of the rechargeable flight time period $|inT_{i,j}^m|$, that is:

$$\Delta E_{i,j}^m = Pr(o_j, o_{i,j}^m) \cdot |inT_{i,j}^m| \tag{7}$$

B. Problem Reformulation

Firstly, we define x_j to denote whether a WSC is placed in grid g_j. If $x_j = 1$, it means there is a WSC in g_j. Otherwise, no WSC is placed in g_j. Secondly, we think that a UAV can receive energy from multiple WSCs from different grids at the same time. Therefore, the energy received by u_i within the k-th path grid g_i^k can be calculated as:

$$\Delta E_i^k = \sum_{j=1}^{|G|} \left(x_j \cdot \Delta E_{i,j}^k\right) \tag{8}$$

where $\Delta E_{i,j}^k$ is energy that u_i received in the k-th rechargeable path grid $g_{i,j}^k$ from the WSC in g_j. Then WDU can be reformulated as:

(P2)

$$\min f(X) = \sum_{j=1}^{|G|} x_j \tag{9}$$

subject to:

$$\begin{cases} ere_i^k \ge E_d \\ ere_i^k \le E_c \end{cases} \tag{10}$$

where

$$x_j \in \{0,1\} \tag{11}$$

$$ere_i^k = sre_i^k + \Delta E_i^k - \mu \cdot \left|T_i^k\right| \tag{12}$$

$$sre_i^k = \begin{cases} ere_i^{k-1}, k > 1 \\ E_0, k = 1 \end{cases} \tag{13}$$

The flight time period that u_i stays in the k-th path grid g_i^k is $T_i^k = [st_i^k, et_i^k]$. sre_i^k denotes the remaining energy of u_i at time st_i^k when u_i enters g_i^k and ere_i^k denotes the remaining energy of u_i at time et_i^k when u_i leaves g_i^k. Then the constraints in (5) is denoted as (10), which ensures that the remaining energy of u_i in each grid is greater than the dropping energy threshold E_d and less than the maximum energy capacity E_c.

In (13), when $k = 1$, g_i^k is the first path grid of u_i and the remaining energy sre_i^k of u_i is equal to the initial energy E_0. Otherwise, sre_i^k equals the remaining energy ere_i^{k-1} when u_i leaves the $(k-1)$-th path grid g_i^{k-1}.

As shown in (12), the remaining energy ere_i^k when u_i leaves the k-th path grid g_i^k equals the remaining energy sre_i^k when u_i enters g_i^k plus the energy ΔE_i^k that u_i received in g_i^k, and minus the energy $\mu \cdot |T_i^k|$ that u_i consumed in g_i^k, where μ is the energy consumption rate of UAVs.

C. Problem Transformation

After problem reformulation, determining the minimal number of WSCs and the location of each WSC is transformed into determining $x_j = 0$ or $x_j = 1$ in each grid $g_j (1 \le j \le |G|)$. Now, we transform WDU (P2) into a BIP problem.

First of all, we define the independent variable matrix X as:

$$X = \left[\begin{array}{cccc} x_1 & x_2 & \cdots & x_{|G|} \end{array}\right]^T \tag{14}$$

The coefficient matrix O of the objective function is set as:

$$O = \left[\begin{array}{cccc} 1 & 1 & \cdots & 1 \end{array}\right]_{1 \times |G|} \tag{15}$$

So, the objective function (9) can be expressed as:

$$\min f(X) = O \times X \tag{16}$$

Next, about the constraint (5), we derive as follows. For the remaining energy ere_i^k of UAV $u_i (1 \le i \le N)$ in the k-th path grid g_i^k, we have:

$$\begin{aligned} ere_i^k &= sre_i^k + \Delta E_i^k - \mu \cdot \left|T_i^k\right| \\ &= ere_i^{k-1} + \Delta E_i^k - \mu \cdot \left|T_i^k\right| \\ &= \cdots \\ &= E_0 + \sum_{k'=1}^{k} (\Delta E_i^{k'} - \mu \cdot \left|T_i^{k\prime}\right|) \end{aligned} \tag{17}$$

So, we have:

$$E_d \le E_0 + \sum_{k'=1}^{k} (\Delta E_i^{k'} - \mu \cdot |T_i^{k'}|) \le E_c \tag{18}$$

That is:

$$\begin{cases} \sum_{k'=1}^{k} \Delta E_i^{k'} \le E_c - E_0 + \sum_{k'=1}^{k} \mu \cdot |T_i^{k'}| \\ \sum_{k'=1}^{k} \Delta E_i^{k'} \ge E_d - E_0 + \sum_{k'=1}^{k} \mu \cdot |T_i^{k'}| \end{cases} \tag{19}$$

The energy that u_i received in all path grids $g_i^k (1 \le k \le K_i)$ is denoted as E_i, then we have:

$$E_i = \begin{bmatrix} \Delta E_{i,1}^1 & \Delta E_{i,2}^1 & \cdots & \Delta E_{i,|G|}^1 \\ \Delta E_{i,1}^2 & \Delta E_{i,2}^2 & \cdots & \Delta E_{i,|G|}^2 \\ \vdots & \vdots & \ddots & \vdots \\ \Delta E_{i,1}^{K_i} & \Delta E_{i,2}^{K_i} & \cdots & \Delta E_{i,|G|}^{K_i} \end{bmatrix} \tag{20}$$

where $\Delta E_{i,j}^k$ is the energy that u_i received in the k-th grid $g_i^k (1 \le k \le K_i)$ from the WSC placed in $g_j (1 \le j \le |G|)$.

In addition, in order to ensure that the remaining energy of each UAV $u_i (1 \le i \le N)$ in each path grid meets the constraint (10), we define the upper bound matrix U_i and lower bound matrix L_i as follows:

$$L_i = \mu \cdot (A_i \times T_i) + (E_d - E_0) \times I_i \tag{21}$$

$$U_i = \mu \cdot (A_i \times T_i) + (E_c - E_0) \times I_i \tag{22}$$

where

$$A_i = \begin{bmatrix} 1 & 0 & \cdots & 0 \\ 1 & 1 & \cdots & 0 \\ \vdots & \vdots & \ddots & \vdots \\ 1 & 1 & \cdots & 1 \end{bmatrix}_{K_i \times K_i} \tag{23}$$

$$T_i = [|T_i^1| \quad |T_i^2| \cdots |T_i^{K_i}|]^T \tag{24}$$

$$I_i = [\begin{array}{cccc} 1 & 1 & \cdots & 1 \end{array}]^T_{K_i \times 1} \tag{25}$$

Next, we define the weight coefficient matrix W_i as:

$$W_i = A_i \times E_i \tag{26}$$

Considering N UAVs in the UAV network, the weight matrix W of the UAV network is defined as:

$$W = \left[\begin{array}{cccc} W_1 & W_2 & \ldots & W_N \end{array} \right]^T \tag{27}$$

The upper bound and lower bound constraint matrix of the UAV network U, L are denoted as:

$$U = \left[\begin{array}{cccc} U_1 & U_2 & \ldots & U_N \end{array} \right]^T \tag{28}$$

$$L = \left[\begin{array}{cccc} L_1 & L_2 & \ldots & L_N \end{array} \right]^T \tag{29}$$

Then, WDU can be transformed into a BIP problem:
(P3)

$$\min f(X) = O \times X \tag{30}$$

subject to:

$$\begin{cases} W \times X \geq L \\ W \times X \leq U \end{cases} \tag{31}$$

So far, WDU is transformed into a BIP problem. By solving P3 to calculate x_j =0 or $x_j = 1$, we can determine whether placing a WSC in each grid $g_j (1 \leq j \leq |G|)$ of Ω and obtain the optimal WSC deployment scheme.

V. Simulation experiments

Based on the actual hardware prototype proposed by GET [30], we proposed our scheme SLTB. However, the wireless UAV charging system of GET has not yet been mass-produced, so we will purchase relevant equipment in the near future and conduct field experiments to verify our model. In this section, we conduct simulation experiments to evaluate SLTB. We compare SLTB with different WSC deployment schemes by analyzing the impact of different parameters on different metrics.

A. Experimental Setup

The experiments are conducted on the extended ONE simulator, in which we added the charging model [25] to model the charging and flight of UAVs. Considering the computational complexity, the BIP problem is solved with the Lagrangean relaxation in [14].

For we are the first to study the WSC deployment problem in the UAV network, to evaluate the performance of SLTB, we first propose a baseline algorithm to select the locations of WSCs randomly (SLR). In SLR, WSCs' are selected randomly to replenish energy for UAVs while the number of WSCs is minimized. Besides, the mobility-aware charger deployment (MACD) in [9] is also used for comparison. Based on the known movement model of end-devices, MACD predicts the candidate locations where the energy of end-devices draining-out may happen, and the grids where those candidate locations locate should be deployed with chargers to prevent the energy draining out. In this paper, the movement model in MACD is replaced by the flight paths of UAVs. The experimental parameters and default values are set based on [9].

TABLE II: Parameters and Default Values

Parameters	Default Values
N	5
v	1m/s
μ	500KJ/ms
E_c	500×10^3KJ
E_0	500×10^2KJ
E_d	10×10^2KJ
e	20m
R	20m

B. Experimental results

In this subsection, we study the impact of 10 parameters on the number of placed WSCs (NoW) in SLTB, SLR, and MACD, namely: the number of UAVs (N), the charging radius of WSCs (R), the charging parameters (α and β), the flight speed of UAVs (v), the energy consumption rate of UAVs (μ), the initial energy of UAVs (E_0), the maximal energy capacity of UAVs (E_c), the dropping energy threshold (E_d) and the edge of grids (discrete granularity e). Multiple experiments are conducted and the average results are discussed below.

1) The impact of N: To evaluate the impact of the number of UAVs N on NoW, we set N from 1 to 6. As shown in Fig. 6a, SLTB outperforms MACD and SLR by 75%, 47.5% respectively. With the increase of N, the placement area becomes larger and more WSCs are needed to replenish energy for more UAVs. From the results in Fig. 6a, we can find that when there are more UAVs in the UAV network, SLTB performs much better than SLR and MACD.

2) The impact of R: To evaluate the impact of the charging radius R of WSCs in the UAV network, when the edge length of grids $e = 25$, we set R as 5m, 12.5m, 20m, 25m, 30m, which discusses 5 different cases between the length of e and R: $2R > \sqrt{2}e, 2R = \sqrt{2}e, \sqrt{2}e > 2R > e, 2R = e, 2R < e$.

As shown in Fig. 6b, our scheme SLTB outperforms MACD and SLR by 78.24%, 44.07% respectively. With the increase of R, the time duration when UAVs can receive energy becomes longer and UAVs can replenish more energy during the flight, so the number of WSCs that the UAV network needs decreases.

3) The impact of α: To evaluate the impact of the charging parameter α in the UAV network, we set α from 150 to 250. As shown in Fig. 6c, SLTB outperforms MACD and SLR by 37.87%, 20.01% respectively. With the increase of α, the received power of each UAV from the WSC increases, so the number of WSCs decreases.

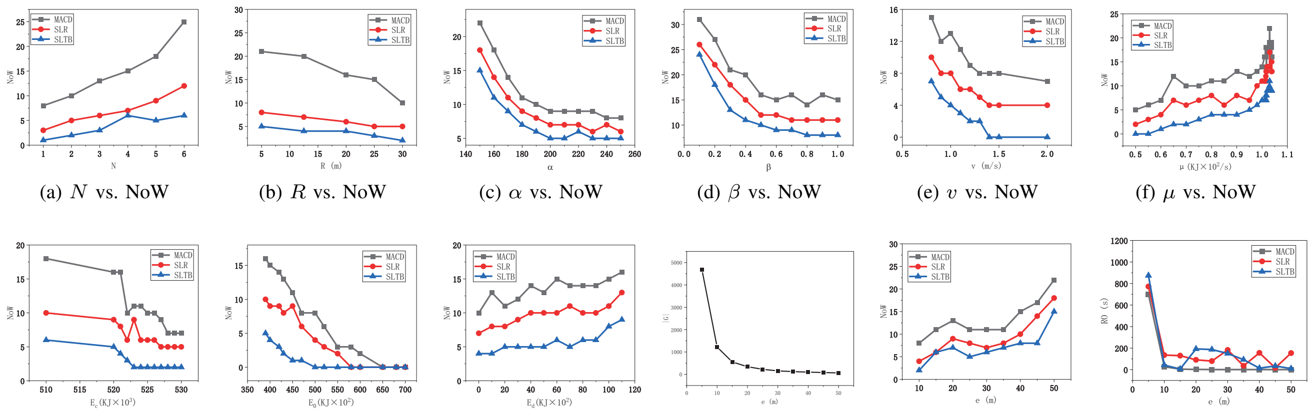

(a) N vs. NoW (b) R vs. NoW (c) α vs. NoW (d) β vs. NoW (e) v vs. NoW (f) μ vs. NoW

(g) E_c vs. NoW (h) E_0 vs. NoW (i) E_d vs. NoW (j) e vs. $|G|$ (k) e vs. NoW (l) e vs. RO

Fig. 6: Experimental results

4) The impact of β: To evaluate the impact of the charging parameter β in the UAV network, we set β from 0.1 to 1. As shown in Fig. 6d, our scheme SLTB outperforms MACD and SLR by 37.36%, 20.33% respectively. With the increase of β, the received power of each UAV from a WSC decreases, so the NoW increases. Besides, as the charging power is nearly proportional to the inverse square of β, the NoW first increases at a fast speed with β, and then increases smoothly.

5) The impact of v: To evaluate the impact of the flight speed v of UAVs, we set v from 0.8m/s to 2m/s. As shown in Fig. 6e, SLTB outperforms MACD and SLR by 78.74%, 66.01%. With the increase of v, the length of flight time decreases, so the energy that UAVs consumed decreases. The faster UAVs fly, the less energy is needed to replenish, so fewer WSCs are needed. Besides, compared with SLR and MACD, SLTB optimizes both the number of WSCs and the location of each WSC, so the WSCs deployed in SLTB are fewer.

6) The impact of μ: To evaluate the impact of the energy consumption rate μ of UAVs, we set μ from 500KJ/s to 1500KJ/s. As shown in Fig. 6f, SLTB outperforms MACD and SLR by 61.63%, 45.61% respectively. With the increase of μ, the energy that UAVs consumed increases and more energy needs to replenish, so the NoW increases.

7) The impact of E_0: To evaluate the impact of the initial energy of UAVs E_0, we set E_0 from 400×10^2KJ to 700×10^2KJ. As shown in Fig. 6h, SLTB outperforms MACD and SLR by 70.63%, 50.61% respectively. With the increase of E_0, less energy needs to be replenished for UAVs, so the NoW decreases. Compared with MACD and SLR, when E_0 keeps increasing, the NoW in SLTB drops to 0 faster.

8) The impact of E_c: To evaluate the impact of the energy maximum capacity of UAVs E_c, we set E_c from 51×10^4KJ to 53×10^4KJ. As shown in Fig. 6g, SLTB outperforms MACD and SLR by 61.63%, 46.61% respectively. With the increase of E_c, UAVs can hold more energy when they are flying and the energy they need to replenish during the flight decreases, so the NoW decreases.

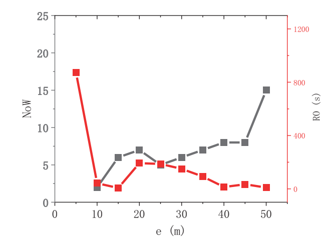

Fig. 7: The impact of e on NoW and RO

9) The impact of E_d: To evaluate the impact of the dropping energy threshold E_d, we set E_d from 0 to 11×10^3KJ. As shown in Fig. 6i, our scheme SLTB outperforms MACD and SLR by 59.56%, 42.28% respectively. With the increase of E_d, the charging request of UAVs becomes more frequent, so, more WSCs are needed to replenish energy.

10) The impact of e: To study the influence of the discrete granularity, we set the edge length of grids e from 1m to 50m. The results are shown in Fig. 6j - Fig. 6l and Fig. 7.

As Fig. 6j shown, with the increase of e, the number of discrete grids $|G|$ decreases gradually. The smaller e is, the more candidate locations of WSCs there will be and the results will be more realistic. However, as shown in Fig. 6l, the longer the SLTB runs as e decreases and the overhead of running (RO) is higher. Fortunately, as shown in Fig. 7, our scheme SLTB can get a good result at a relatively smaller RO, and the number of WSCs in SLTB is reduced by 27% and 48.27% respectively compared to SLR and MACD.

VI. Conclusion

In order to prolong the lifetime of UAVs, this paper studies the problem of WSC deployment in UAV networks (WPU). By determining the minimal number of WSCs as well as the location of each WSC, UAVs can be replenished with the energy they need and do not run out of energy during flight. We first formalize WPU as an optimization problem, which is proved to be NP-hard. Then we propose the scheme of selecting the location of WSCs by transforming WPU into BIP (SLTB). In SLTB, the placement area and flight paths of UAVs are discretized first, and then we present a novel method to reformulate WDU as a BIP problem, which can be solved by existing methods. Finally, experiments are conducted to evaluate that the performance of the SLTB in reducing the number of WSCs.

ACKNOWLEDGMENT

This work is supported by the National Natural Science Foundation of China under Grant No.61402225, the project of Natural Science Research of the Universities of Jiangsu Province (19KJB520012) and the Science and Technology Funds from National State Grid Ltd. (The Research on Key Technologies of Distributed Parallel Database Storage and Processing based on Big Data).

REFERENCES

[1] Jehn-Ruey Jiang and Ji-Hau Liao, "Efficient Wireless Charger Deployment for Wireless Rechargeable Sensor Networks", Energies, Vol.9, No.696, August 2016

[2] Y. Chen and J. Jiang, "Particle Swarm Optimization for Charger Deployment in Wireless Rechargeable Sensor Networks," 2016 26th International Telecommunication Networks and Applications Conference (ITNAC), 2016, pp. 231-236, doi: 10.1109/ATNAC.2016.7878814.

[3] H. Dai et al., "Radiation Constrained Wireless Charger Placement," in IEEE/ACM Transactions on Networking, vol. 29, no. 1, pp. 48-64, Feb. 2021, doi: 10.1109/TNET.2020.3028704.

[4] H. Dai, C. Wu, X. Wang, W. Dou and Y. Liu, "Placing Wireless Chargers with Limited Mobility," IEEE INFOCOM 2020 - IEEE Conference on Computer Communications, 2020, pp. 2056-2065, doi: 10.1109/INFOCOM41043.2020.9155356.

[5] N. Yu, H. Dai, G. Chen, A. X. Liu, B. Tian and T. He, "Connectivity-Constrained Placement of Wireless Chargers," in IEEE Transactions on Mobile Computing, vol. 20, no. 3, pp. 909-927, 1 March 2021.

[6] T. Lin, S. Li, H. Chang, W. Chang and Y. Lin, "An Effective Wireless Charger Deployment Method for Complete Coverage in Wireless Chargeable Sensor Networks," 2016 International Conference on Networking and Network Applications (NaNA), 2016, pp. 379-382.

[7] S. Sudevalayam and P. Kulkarni, "Energy harvesting sensor nodes: Survey and implications," IEEE Commun. Surveys Tuts., vol. 13, no. 3, pp. 443–461, 2011.

[8] S. He, J. Chen, F. Jiang, D. K. Yau, G. Xing, and Y. Sun, "Energy provisioning in wireless rechargeable sensor networks," IEEE INFOCOM, pp. 2006–2014, Apr. 2011.

[9] T.-C. Chiu et al., "Mobility-aware charger deployment for wireless rechargeable sensor networks," in IEEE APNOMS, 2012, pp. 1–7

[10] Y. Li, Y. Chen, C. S. Chen, Z. Wang and Y. Zhu, "Charging While Moving: Deploying Wireless Chargers for Powering Wearable Devices," in IEEE Transactions on Vehicular Technology, vol. 67, no. 12, pp. 11575-11586, Dec. 2018.

[11] Y. Zhu, X. Tian, K. Chi, C. Wen and Y. Zhu, "Real-Time Power Control of Wireless Chargers in Battery-Free Body Area Networks," 2019 IEEE Global Communications Conference (GLOBECOM), Waikoloa, HI, USA, 2019, pp. 1-6.

[12] S. He, J. Chen, F. Jiang, D. K. Y. Yau, G. Xing, and Y. Sun, "Energy provisioning in wireless rechargeable sensor networks," IEEE Trans. Mobile Comput., vol. 12, no. 10, pp. 1931–1942, Oct. 2013.

[13] S. Zhang, Z. Qian, F. Kong, J. Wu, and S. Lu, "P^3: Joint optimization of charger placement and power allocation for wireless power transfer," in Proc. IEEE Conf. Comput. Commun. (INFOCOM), Apr. 2015, pp. 2344–2352.

[14] İ. Kuban Altınel, Necati Aras, Evren Güney, Cem Ersoy, "Binary integer programming formulation and heuristics for differentiated coverage in heterogeneous sensor networks," Computer Networks, Volume 52, Issue 12, 2008, Pages 2419-2431.

[15] H. Shakhatreh, A. H. Sawalmeh, A. Al-Fuqaha, Z. Dou, E. Almaita,I. Khalil, N. S. Othman, A. Khreishah, and M. Guizani, "Unmanned aerial vehicles (UAVs): A survey on civil applications and key research challenges," IEEE Access, no.7, pp.48572–48634, 2019.

[16] A. BoggioDandry and T. Soyata, "Perpetual flight for uav drone swarms using continuous energy replenishment, IEEE Annual Ubiquitousv Computing," Electronics Mobile Communication Conference (UEMCON), pp.478–484, 2018.

[17] X. Dong, Y. Ren, J. Meng, S. Lu, T. Wu and Q. Sun, "Design and Implementation of Multi-rotor UAV Power Relay Platform," 2018 2nd IEEE Advanced Information Management, Communicates,Electronic and Automation Control Conference (IMCEC), Xi'an, 2018, pp. 1142-1146.

[18] J. Leonard, A. Savvaris, and A. Tsourdos, "Energy management in swarm of unmanned aerial vehicles," International Conference on Unmanned Aircraft Systems (ICUAS), pp.124–133, 2013.

[19] D. Arivudainambi and S. Balaji, "Optimal placement of wireless chargers in rechargeable sensor networks," IEEE Sensors, vol. 18, no. 10, pp. 4212-4222, 2018.

[20] L. Xie, Y. Shi, Y. T. Hou, and A. Lou, "Wireless power transfer and applications to sensor networks," IEEE Wireless Communications, vol. 20, no. 4, pp. 140–145, 2013.

[21] G. Jiang, S. Lam, Y. Sun, L. Tu, and J. Wu, "Joint charging tour planning and depot positioning for wireless sensor networks using mobile chargers," IEEE/ACM Transactions on Networking, vol.25, no.4, pp.2250–2266, 2017.

[22] C. Lin, J. Zhou, C. Guo, H. Song, G. Wu and M. S. Obaidat, "TSCA: A Temporal-Spatial Real-Time Charging Scheduling Algorithm for On-Demand Architecture in Wireless Rechargeable Sensor Networks," in IEEE Transactions on Mobile Computing, vol. 17, no. 1, pp. 211-224, 1 Jan. 2018.

[23] Z. Fan, Z. Jie and Q. Yujie, "A Multi-Node Rechargeable Algorithm via Wireless Charging Vehicle with Optimal Traveling Path in Wireless Rechargeable Sensor Networks," 2018 ICUFN, Prague, 2018, pp. 531-536.

[24] T. Liu, B. Wu, S. Zhang, J. Peng and W. Xu, "An Effective Multi-node Charging Scheme for Wireless Rechargeable Sensor Networks," IEEE INFOCOM 2020 - IEEE Conference on Computer Communications, Toronto, ON, Canada, 2020, pp. 2026-2035.

[25] A. P. Sample, D. J. Yeager, P. S. Powledge, A. V. Mamishev, and J. R. Smith, "Design of an RFID-based battery-free programmable sensing platform," IEEE Transactions on Instrumentation and Measurement, vol.57, no.11, pp.2608–2615, 2008.

[26] L. Fu, P. Cheng, Y. Gu, J. Chen, and T. He, "Optimal charging in wireless rechargeable sensor networks," IEEE Transactions on Vehicular Technology, vol.65, no.1, pp.278–291, 2016.

[27] T. M. Cabreira, C. D. Franco, P. R. Ferreira and G. C. Buttazzo, "Energy-Aware Spiral Coverage Path Planning for UAV Photogrammetric Applications," in *IEEE Robotics and Automation Letters*, vol. 3, no. 4, pp. 3662-3668, Oct. 2018.

[28] Z. Lv, L. Yang, Y. He, Z. Liu and Z. Han, "3D environment modeling with height dimension reduction and path planning for UAV," 2017 9th International Conference on Modelling, Identification and Control (ICMIC), 2017, pp. 734-739, doi: 10.1109/ICMIC.2017.8321551.

[29] Y. Wang, H. Wang and Y. Lun, "Shortest Path Planning of UAV for Target Tracking and Obstacle Avoidance in 3D Environment," 2020 39th Chinese Control Conference (CCC), 2020, pp. 3385-3390.

[30] Global Energy Transmission Corporation, http://getcorp.com/ (accessed 11 June 2021)

[31] Webit Festival Europe on May 15, 2019, http://getcorp.com/getcorp-at-webit-festival-europe-2019/ (accessed 11 June 2021)

[32] GET In-flight wireless charging, https://www.youtube.com/watch?v=DvNWkugbO-k (accessed 11 June 2021)